On the limit: Estimating round baler torque for grass harvesting scenarios

Computers and Electronics in Agriculture 232 (2025) 110056

Contents lists available at ScienceDirect

Computers and Electronics in Agriculture

journal homepage: www.elsevier.com/locate/compag

Original papers

On the limit: Estimating round baler torque for grass harvesting scenarios

Tomás Crotty [a], John Warren [b], Conor Shanahan [b], Edward Jones [a], Martin Glavin [a], Dallan Byrne [a,*]

[a] Electrical and Electronic Engineering, School of Science and Engineering, University of Galway, Galway, Ireland
[b] McHale Engineering Unlimited Company, Ballinrobe, Mayo, Ireland

ARTICLE INFO

Keywords:
Agricultural machinery
Baling
Force estimation
Remaining useful life
Signal processing

ABSTRACT

This paper introduces a novel, cost-effective approach to measure loading torque on an agricultural baler implement. Round balers gather grass fodder and form cylindrical bales, which are subsequently used for feeding livestock. As fodder accumulates within the bale chamber, the torque on the drive shaft increases, necessitating an increase in input power. The operator must manage the loading levels to prevent excessive strain on implement components and avoid a breakdown. State-of-the-art torque measurement techniques are difficult to integrate into harvesting implements due to their significant cost and mechanical footprint. Consequently, baling implements lack loading measurement capabilities, forcing operators to gauge power draw without quantitative feedback.

This paper proposes a sensor solution to approximate torque on a round baler, significantly reducing costs when compared to existing methods. The approach correlates chain stress throughout bale formation by monitoring deformation of the chamber drive chains. Measurements were acquired from a fixed-chamber baler-wrapper with ground-truth torque benchmark recordings. Experiments were carried out using artificial loading on a static machine and then within the field, with a mobile implement forming grass silage bales. A prototype sensor was installed on a grass harvesting contractor's baler-wrapper to examine performance across a single season, across 180 sites in the West of Ireland. Results from each scenario highlight a linear relationship between sensor and ground-truth torque measurements. The method achieved a 7% mean peak torque estimation error, allowing operators to monitor mechanical loading limits during bale formation and to increase efficiency in grassland agricultural processes.

1. Introduction

Grass forage is harvested during periods of rapid growth, to later feed housed animals during winter when growth slows significantly and ground conditions deteriorate (Wilkinson, 1981; Muck and Shinners, 2021; Van Middelaar et al., 2014). Balers are widely used to collect cut forage and form it into a bale, where the bale may be wrapped to promote anaerobic fermentation when crops present with a significant moisture content (Finch et al., 2014; Genever, 2019).

Operating bale harvesting machinery requires experienced operators and can incur substantial maintenance expenses (Buckmaster, 2003). Considering that over 60% of EU farms are smaller than 5 Hectares, it is not economically viable for every farm to purchase and run their own machinery (Grandovska et al., 2018). Consequently, many European farms rely on third-party contractors or agricultural cooperatives to supply the necessary equipment and expertise to efficiently harvest forage for several clients within a limited time-span (Parvin et al., 2022).

Forage harvesting machinery must be well maintained and regularly serviced, particularly in a contracting scenario where a limited number of machines serve multiple farmers. As a result, these machines are subjected to significant stress during operation and their parts can rapidly wear out or break, without prior warning. When a contractor's harvesting implement breaks down, it not only impacts the current client and their crops, it will have a knock-on affect on subsequent jobs where harvesting must be completed within a period of time prior to crop degradation or the onset of precipitation (Muck and Shinners, 2021).

In round bale harvesting, the implement power is drawn through the tractor Power Take Off (PTO) drive and allocated, via a split-drive gearbox to the crop pickup mechanism and the bale formation chamber. The power consumption can be measured as torque on the driveline shafts of the baler. As the fixed chamber fills with fodder, the power consumption of the implement increases proportionally to

* Correspondence to: Alice Perry Engineering Building, University of Galway, Galway, Ireland.
E-mail address: dallan.byrne@universityofgalway.ie (D. Byrne).

https://doi.org/10.1016/j.compag.2025.110056
Received 4 September 2024; Received in revised form 22 January 2025; Accepted 28 January 2025
Available online 14 February 2025
0168-1699/

the mass of fodder rotating in the chamber (Lei and Wang, 2021). When a significant mass of fodder is collected, a blockage can occur at the pickup unit when the majority of available power is drawn by the chamber, causing the implement components to stall. In this scenario, an overload or slip clutch will disengage the PTO driveline from the implement in order to prevent excessive damage to the baler components (Nienhaus, 2012; Regler et al., 2023). Despite overload protection, repeated exposures to excess torque can permanently damage crucial implement components. A baler operator will qualitatively gauge the power consumption of the implement, to avoid unwanted stoppages and protect the machine components.

A sensing modality can be employed to provide quantitative feedback to the operator. A ferromagnetic sensor can be used to accurately measure the torque of a rotating shaft by monitoring the frequency properties of ferromagnetic films within the sensor (Beirle and Seemann, 2020). Ferromagnetic shaft sensors are relatively expensive, often costing over €5000 (NCTE AG, 2020). Electric drive motor power and speed can be used to indirectly estimate motor torque, however, this technique can only be used for electric drive systems and inaccuracies can occur due to power losses (Brüel and Kjær, 2022).

The literature contains several examples illustrating the approximation of torque and power levels of agricultural machinery. Mohsenimanesh et al. (2015) used hydraulic pressure sensors and inductive proximity sensors to estimate feedroll and header torque of a forage harvester. Mohsenimanesh et al. (2015) measured the pressure and motor speed at the input and output of both elements of a pull-type forage harvester. Using hydraulic pressure and inductive proximity sensors, the estimated output power yielded R^2 values of up to 0.97 when correlated with crop throughput, where R^2 is the coefficient of determination between two groups of independent variables.

Hofstetter and Liu (2011) examined the power requirements of a square baler when compressing corn stover, indian grass, wheat straw and switchgrass crops. The study highlighted how compression pressure requirements increased when the feed density and compression speed increased. Power requirements increased by up to 73%, when the compression of switchgrass was compared with wheat straw. Fasick and Liu (2020) studied the power consumption in a square baler when baling unconditioned and conditioned miscanthus crop. The lab-based results showed that peak force requirements during bale compression reduced from 12kN to 7.55kN when baling unconditioned miscanthus compared with conditioned miscanthus.

Intellectual property in the round baler domain has included reference to torque measuring devices on the belt baler driveshaft components (Wilkens et al., 2002; Hoffmann, 2018). Rubber belts are used within the baling chamber of a belt baler to maintain the shape of the bale where the diameter can be altered by repositioning the belt rollers (McHale et al., 2024). A device outlined in Wilkens et al. (2002) allows the baling implement to slacken chamber belts as the measured torque increases close to the slip clutch threshold torque. A patent granted to Hoffmann (2018) describes two sensors that measure torque on the bale formation and bale feeding driveshafts.

Silage bales can present with significant moisture content and weigh in excess of 700 kg (Keles et al., 2009). Each time a bale is formed, a significant amount of chamber torque is registered, often exceeding 2000 Nm on a 540 Revolutions Per Minute (RPM) rotating shaft. The force is distributed from the PTO driveshaft, to the pickup unit and the bale chamber of the baler using roller chains, where the aforementioned are highlighted on a Fusion 3+ combination baler wrapper in Fig. 1. Initially, when the bale Chamber (CR) is relatively empty and the Pickup Unit (PU) feeds the grass from the ground swath. As there is a limited mass of fodder within the CR, the PU loading reflects the total loading of the system, or torque on the PTO (τ_{PTO}). As the CR fills, the chamber rollers must rotate a significant mass of fodder and will generate the majority of the implement loading. Peak bale cycle torque (τ_{PK}) is generally observed at the end of the bale formation sequence, prior to bale netting.

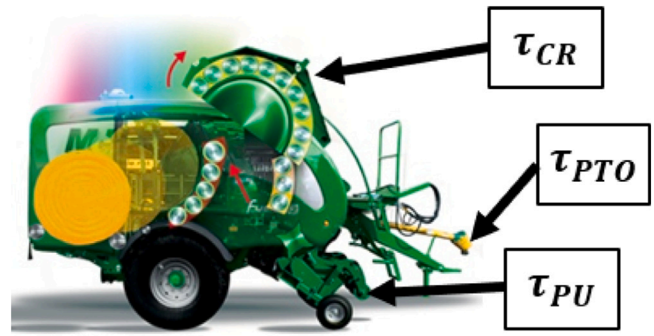

Fig. 1. Labelled image of McHale Fusion 3+ fixed size chamber baler-wrapper.

Chain systems transmit power from the main drive-system to the CR and PU units of the baler. These "Roller" chains, are comprised of two parallel rows of inner and outer plates (Niijjaawan and Niijjaawan, 2010). They distribute power across a system using sprockets (Otoshi et al., 1995). These sprockets, commonly known as drive sprockets, provide power to the drive chain (Lyons et al., 2016). The sprocket teeth typically have an inclination that allows the chain rollers to engage and slip off the sprocket freely (Otoshi et al., 1995). Pins and bushings connect the parallel rows of plates with the pin moving freely inside the bushing (Niijjaawan and Niijjaawan, 2010). The "Roller" surrounds each bush and turns freely (Cory, 2005) causing the chain to manoeuvre with the sprocket during motion. This allows the chain to operate at relatively higher speeds than chains that do not contain roller pins (Lyons et al., 2016). Roller chains, when maintained properly, can operate at efficiencies up to 98% in ideal conditions (Niijjaawan and Niijjaawan, 2010).

The implement chains undergo an elastic elongation when placed under load, whereby a temporary effect is observed (Otoshi et al., 1995). After repeated use and periods of elastic elongation, the bushings surrounding the chain pins wear away over time, particularly when the machine comes under considerable cyclic loads and significant torque levels. This causes excessive wear on the pins and bushing elements of a roller chain which leads to permanent (plastic) elongation of the chain over time (Otoshi et al., 1995). As a result, it is advised to replace the chain after approximately 10000 bale cycles to avoid critical fatigue failure in the chain and reduce the risk of slippage on the sprockets.

This paper introduces a method for estimating the torque experienced under load in a fixed chamber baler by measuring the elastic stretch of the baler drive chain. This paper contributes to the state-of-the-art with:

- An experimental analysis of the relationship between baler chamber chain drive elastic stretch and baler chamber torque;
- A novel method to estimate baler torque using elastic stretch measurements based on data collected during the 2020 forage harvesting season.

Several bench and in-field tests were performed on the baler. Unsupervised measurements were obtained over a full harvesting season, from a fixed chamber baler used by a contractor in Galway, Ireland.

This paper demonstrates a linear relationship between chain elastic stretch parameters and machine torque in all tests completed with R^2 values between .88 and .99. Peak machine loading can be approximated with an average error of 5% when using the proposed technique.

The paper is organized as follows: Section 2 describes the machinery apparatus, experiment design and methods of data acquisition employed throughout testing. Section 3 describes the results generated during bench, in-field and season long testing. Finally, conclusions are described in Section 4.

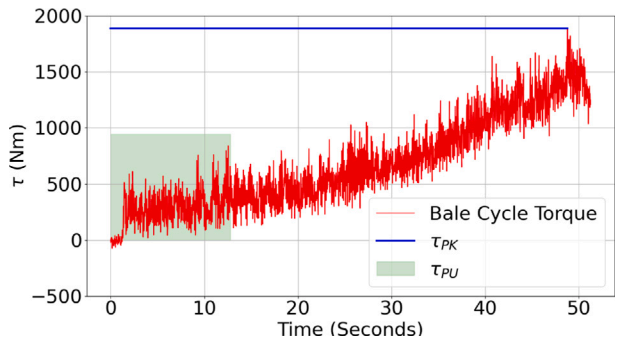

Fig. 2. Baler torque for one bale cycle.

2. Materials and methods

The section will first provide an overview of the novel approach to measuring temporary (elastic) and permanent elongation of a drive chain. The measurement hardware and environment will then be described and three data acquisition scenarios will be presented.

2.1. Proposed method

2.1.1. Loading during the bale-formation cycle on a fixed chamber baler implement

During a harvesting operation, crop is gathered by a fixed chamber baler and fed through to a chamber of fixed diameter, where rollers are positioned along the curved surface. The baler is powered from a spinning PTO shaft, rotating at either 540 or 1000 RPM. Mechanical power is transmitted from the shaft through a gearbox, which is then distributed to two chain-driven systems:

1. A Rotary Pick-Up (PU) unit that drives a rotating shaft with protruding tynes that lift crop from the ground and feed it through to the bale chamber.
2. A set of Chamber Rollers (CR) that rotate and compress the collected crop in a cylindrical chamber as shown in Fig. 1.

A torque loading graph for a sample bale cycle is shown in Fig. 2. As illustrated in Eq. (1) and Fig. 1, PTO torque (τ_{PTO}) is comprised of PU torque (τ_{PU}) and CR torque (τ_{CR}). In the initial phase of the bale cycle, the majority of the load torque is generated by the PU unit while the quantity of grass in the bale formation chamber is low, as shown in the green shaded region in Fig. 2. As the crop mass inside the chamber increases, the loading torque is then increasingly influenced by the CR as the torque magnitude increases over time. The time when the bale chamber is fully packed with grass and registered PTO torque is at its peak is illustrated by the vertical blue line in Fig. 2. At this point, the PU unit is still contributing to the torque on the tractor PTO shaft, however the CR unit may contribute up to 90% of the overall implement loading, when the bale cycle torque is at its peak (τ_{PK}). The relationship between τ_{PTO}, τ_{CR} and τ_{PU} is described as:

$$\tau_{PTO} = \tau_{PU} + \tau_{CR} \tag{1}$$

A slip clutch will act as a torque limiting device, defining an upper threshold of implement loading. At the peak of the bale formation cycle, shown in Fig. 2, the CR contains a significant mass of crop and will contribute to the majority of τ_{PTO}, limiting the torque available at the PU unit. If a large amount of crop presents at the PU, the additional loading may cause the overall torque limit to be exceeded, triggering the slip clutch and causing the machine driveline to disengage. A real-time feedback mechanism to relay τ_{CR} to the operator would allow them to alter their driving style to avoid an excess of τ_{PTO}, and maintain baling in an uninterrupted manner.

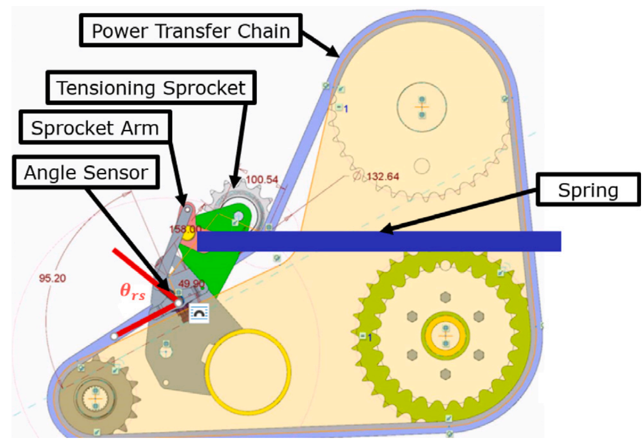

Fig. 3. Labelled model of the baler CR drive chain system constructed using Pro Engineer/PTC Creo.

2.1.2. Torque approximation system

The paper proposes to estimate τ_{CR} in (1) by examining the elastic elongation of the main drive chain within the baling implement. To describe the main drive of the Fusion 3+ baler-wrapper implement, an engineering model of the CR drive chain system was constructed using Creo Pro Engineer (Creo, 2022) CAD design software, as shown Fig. 3. As the chain pins and bushings wear throughout the baling season, the chain will experience a permanent elongation. During the formation of a single bale, τ_{CR} causes elastic elongation or "stretch" of the chain components, that return to their original length after the bale is released from the chamber. The authors propose to measure this elastic elongation, by monitoring the movement of a tensioning sprocket arm held in place using a tension spring highlighted in blue in Fig. 3.

A rotary sensor is mechanically attached to the sprocket arm which registers an angle between $\frac{\pi}{6}$ and $\frac{5\pi}{6}$ radians. The angle can be translated to a linear displacement by:

$$d_h = l_{rs}\left(\tan\left(\frac{\pi}{2} - \theta_{rs}\right)\right) \tag{2}$$

where d_h represents the horizontal displacement (in m) at the tip of the rotary sensor arm, the length of the rotary arm is l_{rs} and θ_{rs} is the angle on the rotary sensor.

2.1.3. Modelling analysis of chain length

The engineering model of the CR drive chain system shown in Fig. 3 was used to evaluate the relationship between chain length and the proposed rotary angle sensor which was connected to the tension sprocket using a dynamic bracket. This chain transfers power from the output of the main PTO gearbox to the CR unit. The power transfer chain length was adjusted to move the location of the tensioning sprocket and, in-turn, change the value of θ_{rs} in the design in Fig. 3. Results from this simulation provided the correlation between tensioning sprocket movement measured by a rotary angle sensor and chain length. d_h calculations in (2) account for the angular movement on one sprocket in the main chain drive system, while the elastic elongation of the chain (ee_{chain}) accounts for the movement of all sprockets in the chain drive system and shows the effect they have on chain length. ee_{chain} is defined as the length the drive chain elastically elongates to during each bale cycle, with the chain length at the initial idle stage of the bale cycle having an ee_{chain} value of 0.

2.2. Experimental setup

2.2.1. Static implement experiments

Grass growth is limited throughout the winter months, particularly in an inclement climate (Wilkinson, 1981). To facilitate data collection

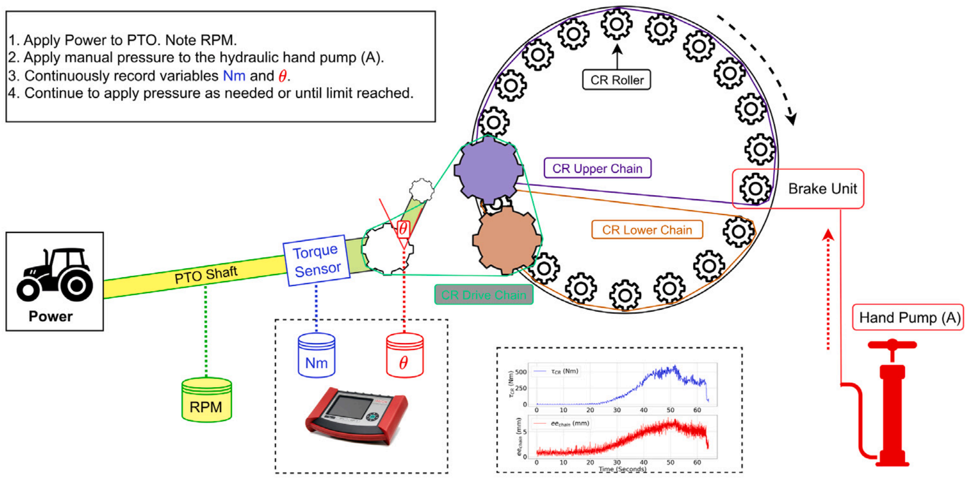

Fig. 4. Experimental setup for the static implement tests. Power was applied from a tractor, torque was measured from an NCTE sensor on the PTO shaft, and torque was induced using a car brake, hydraulically activated through a manual pump. The Chamber (CR) is shown along with the rolling cylinder gears. Hydraulic pressure is applied to the hand pump (A) to activate the brake on the roller (shown in Fig. 5). The torque (Nm) and tensioning sprocket angle sensor (θ) are recorded using a Hydac HMG4000 sensor logging device.

Fig. 5. Car brake attached to baler CR roller to apply load during static indoor testing.

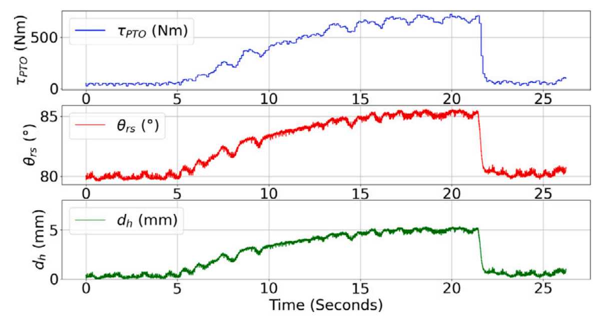

Fig. 6. Torque and rotary sensor static indoor test results for one static indoor loading cycle using chain A.

during these months, a workshop-based loading system was designed to induce torque on a static 2021 McHale Fusion 3+ baler-wrapper, as illustrated in Fig. 1. The main PTO gearbox on the implement was designed for a 1000RPM input. Loading was achieved by attaching a 2002 Mercedes Vito hydraulic brake unit, where the brake rotor was connected to a single roller element of the CR unit, as shown in Fig. 5. Braking was induced through a manual hydraulic pump, at the side of the fixed chamber baler, inducing load on the CR. The rotary sensor was attached to the tensioning sprocket described in Section 2.1.2. To obtain τ_{CR}, a ground truth torque measurement was acquired with a 3000 Nm NCTE torque sensor (NCTE AG, 2020), attached to the PTO shaft between the tractor and fixed-chamber baler. The PU was rotating, however, the torque loading from the PU was negligible as no crop was present in this static indoor test. A block diagram, illustration the experimental setup is shown in Fig. 4.

Several experiments were completed on three different chains:

- Chain A — A Diamond 100H (Diamond-Drives, 2024) chain of length 2888 mm that was used to make 3000 bales prior to testing;
- Chain B — An unused Diamond 100H chain of length 2882 mm;
- Chain C — Chain B extended with an extra link, measuring 2900 mm in length.

A tractor was used to apply PTO power to the baler. Sensor measurements were recorded on a Hydac HMG4000 data acquisition unit (HYDAC, 2022) and the implement was loaded by pumping the brake. An example of the recorded data is shown in Fig. 6 for a single CR loading scenario with chain B. A maximum τ_{CR} of 2668 Nm was generated using the brake unit. All torque measurements in this paper are presented in relation to τ_{PTO}, where the gear ratio on the CR unit is used to present torque in relation to τ_{PTO} instead of τ_{CR}.

2.2.2. In-field implement baling experiments

A field experiment was carried out to evaluate the proposed system on a working machine producing grass silage bales. The study took place in Ballinrobe, County Mayo, Ireland on the 9th of September 2021. A McHale Fusion 3+ fixed chamber baler-wrapper was used, towed by a 2017 Fendt 718 Vario tractor delivering a gross 135 kW of power. 42 wrapped silage bales were produced, where the operator settings were adjusted to produce a range of peak torque loadings within the field:

- The output bale diameter was varied between 1.05 m and 1.35 m through a Fusion 3+ controller display setting. An increase of diameter would result in a relative increase in mass, compared to a smaller bale and therefore increase the relative torque loading;

- The desired bale density was modified (between minimum and maximum) on the Fusion 3+ controller display. When the CR diameter was fixed, the increase in density will contribute to a relative increase in torque loading on the CR;
- The operator modified their tractor ground speed between each bale produced. If the speed of the implement is increased, there is a larger volume of crop entering the machine for a given time period. This extra mass can cause significant spikes in CR torque, and on-occasion may trigger the implement overload clutch.

A ground truth torque sensor was attached to the CR cardan shaft on the baler, to isolate the loading measurement from the PU system. 13 knives were engaged in the chopper unit for each bale. Bale weights varied between 593 kg and 786 kg. A Hydac HMG 4000 was used to record the ground truth torque and rotary sensor data.

2.2.3. Measurements over a full silage harvesting season

To examine the chain characteristics and subsequent baler loading over a significant duration, the proposed system was trialled on a 2013 McHale Fusion 3+ fixed chamber baler-wrapper between May and October 2020. The baler was towed by a 2016 John Deere 6170R tractor with a gross power output of 127 kW. The machinery was owned by a harvesting contractor who leases operators and harvesting equipment to clients. Only grass silage baling was considered in this observation study. All data collected for this evaluation was done so without any author supervision or influence. The season-long harvest data was then used to estimate baler torque.

A rotary angle sensor was used to measure bale chamber power transfer chain horizontal displacement throughout harvesting. A ground-truth sensor was attached to the main PTO shaft measuring τ_{PTO}, as shown in Fig. 1. The ground truth measurements contained contributions from τ_{CR} and τ_{PU}, as highlighted in Eq. (1). Attaching a ferromagnetic sensor to the cardan shaft of the chamber drive would have required significant mechanical alteration, which was infeasible due to the time constraints that present when using contractor machinery.

A GNSS module was used to obtain positioning, time and displacement data, similar to the methods described in Balmos et al. (2022). An EMLID Reach M+ GNSS module (Emlid, 2020), containing a Ublox NEO-M8 chip (U-Blox, 2020) was used to record geolocation coordinates. A TW44221-00 Tallysman wideband Dual Feed, 1.574 GHz - 1.606 GHz antenna (Calian Advanced Technologies, 2020) was integrated and placed on the roof of the tractor. Coordinates were measured at a rate of 2 Hz. Proprietary McHale messages and sensor data were transmitted over a CANbus network from a customized ECU on the fixed chamber baler, while several Isobus (Brodie et al., 2023) measurements of tractor parameters were recorded. All GNSS and J1939 packets were received, parsed into time, sensor value and sensor name data and stored locally in a document based database operating on an 8th generation Intel Nuc (Intel i3 processor and 4 GB of RAM) running Ubuntu 16.04. All coordinate and measurement timestamps were logged in UTC format (Harkin et al., 2024).

The data was pre-processed to extract time-series data corresponding to a bale formation sequence.

- The individual fields or job-sites were identified and the corresponding data was isolated according to the work methods outlined by Harkin et al. (2024).
- Bale formation sequences were identified as the time between individual transfer sequences, from the formed bale in the CR to the wrapping tray, at the rear of the combi baler-wrapper. The first bale formed in each field was not included in the study as the start time could not be determined through automated scripting.
- Measurements during static periods, when the implement was idle, were removed. Bale sequences were only included if there was no temporal break in measurement timestamps, where the measurements presented with consistent sampling rates between bale transfers.

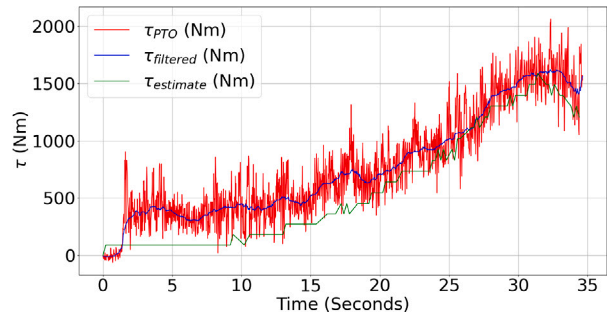

Fig. 7. Measured baler torque (τ_{PTO}), median filtered baler torque ($\tau_{filtered}$) and estimated torque ($\tau_{estimate}$) for one bale formation sequence from the full silage harvesting season.

After pre-processing, there were 3001 valid bale cycles available for analysis. Chain length was calculated for each valid bale cycle using rotary angle sensor data. Chain length and processed torque were then correlated for each valid bale cycle captured during the harvesting season.

Throughout the season, the ground truth torque measurements were taken from the tractor PTO (τ_{PTO}), and included contributions from both τ_{PU} and τ_{CR}. The presence of τ_{PU} contributed to amplitude fluctuations in torque readings. To counter this, a median filter was applied to τ_{PTO} for each of the 3001 bale sequences, generating the ground-truth filtered signal $\tau_{filtered}$ shown in Fig. 7.

A torque-chain length relationship was calculated through an Ordinary Least Sqaures (OLS) method and this correlation was then used to estimate baler torque using chain length data. The slope and intercept can be described as:

$$\tau_{estimate} = \left((m \times e_{pk}) + C\right) \tag{3}$$

Where $\tau_{estimate}$ represents the estimated peak median filtered torque of the bale cycle. Slope m and intercept C are constant for each bale cycle and are found using the line of best fit, while e_{pk} is the peak elongation of the main drive chain for the bale cycle.

The following metrics were used to benchmark $\tau_{estimate}$:

- Bale cycle error:
  - The mean error between $\tau_{filtered}$ and $\tau_{estimate}$ is calculated across the entire bale cycle, from time $t = 0$ to T, where T is the maximum bale cycle duration, in seconds.
- Bale compaction period error:
  - The average error between $\tau_{filtered}$ and $\tau_{estimate}$ is calculated from $2T/3$ to T.
- Torque peak error:
  - The maximum value of $\tau_{estimate}$ is calculated for each bale cycle and is compared with $\tau_{filtered}$ at the same time instance.

Once each metric is calculated, for an individual bale formation sequence, the results are aggregated across the entire dataset, where the overall mean and median of the metrics are presented in Section 3.4.3.

3. Results and discussions

The results section is split into subsections examining: modelling analysis of chain length, the static experiment with artificial load results, in-field experiment results, full silage harvesting season results and, finally, all three data acquisition scenarios are compared.

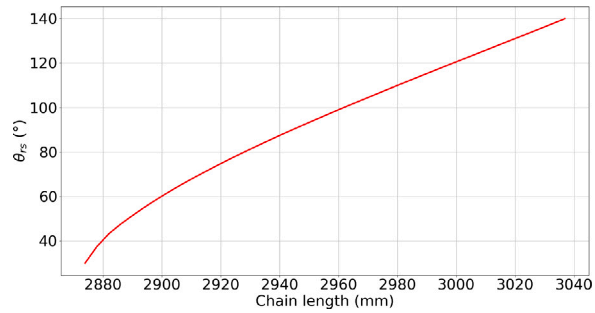

Fig. 8. Results from CAD design model, where the chain length on the X axis is modified to cause a change in θ_{rs} on the Y axis, illustrating the relationship between rotary sensor angles and the change in main chain drive length due to elastic elongation.

3.1. Modelling analysis of chain length

An engineering model of the CR drive chain system was constructed as described in Section 2.1.3 and as shown in Fig. 3. The model allowed the authors to modify the chain length and observe the variations in angle measurements on the chain sprocket. The relationship between θ_{rs} and chain length found using the model are illustrated in Fig. 8. This allowed rotary sensor data to be illustrated as the elastic elongation of the chain (ee_{chain}) as in Section 2.1.3.

3.2. Static experiment with artificial load results

In this section, the study examines the effect of inducing load on a static fixed chamber baler CR as described in Section 2.2.1, and the relationship between the baler torque and the movement of the sprocket arm used to tension the main chain drive, shown in Fig. 5.

Figs. 9(a), 9(b) and 9(c) illustrate peak τ_{PTO} displacement correlated with peak horizontal displacement calculated using movement of the sprocket arm. Several static artificial load cycles were completed with chain A (Fig. 9(a)), chain B (Fig. 9(b)) and chain C (Fig. 9(c)) used as the main chain drive. The results for the three chains tests are presented on a single graph for comparison, in Fig. 10.

The graphs correlate movement of the sprocket arm used to tension the main chain drive with baler torque for each test completed. The OLS fit for each chain experiment completed registers an R^2 coefficient of greater than or equal to 0.98, which is significant. When results from all three chain experiments are combined an R^2 of 0.98 is still achieved.

As the movement of the sprocket arm maintains the tension on the main drive chain, static experiment results show that the rotary sensor arm moves horizontally, in proportion with the increase of τ_{PTO} during static testing. The strong correlation illustrates a relationship between d_h (Eq. (2)) and torque despite using three different chains each with a varying level of aging (permanent elongation) during these experiments. Static experiments, however, apply artificial load to a single baler chamber roller, whereas in a field baling scenario, the load would be distributed across more rollers in the chamber possibly influencing how the main drive chain behaves during the cycle.

Using the relationship between rotary sensor angle values and the main chain drive length, as illustrated in Fig. 8 and described in Section 3.1, Fig. 11 highlights how the simulated chain elastic elongation ee_{chain} correlates with τ_{PTO} in the experiments described in Section 2.2.1.

The OLS fit for each test completed, using ee_{chain} (instead of d_h) registers, an R^2 coefficient of greater than or equal to 0.97. This illustrates the relationship between τ_{CR} and modelled chain length during static experiments with artificial load analysis. In-field implement baling experiments were then carried out to examine the elastic properties of the main drive chain during the gathering of grass crop.

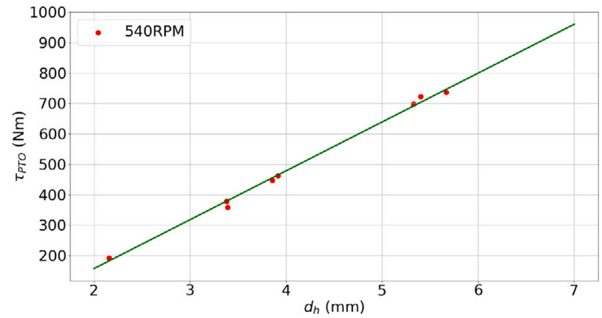

(a) Chain A (R^2 = 1.0).

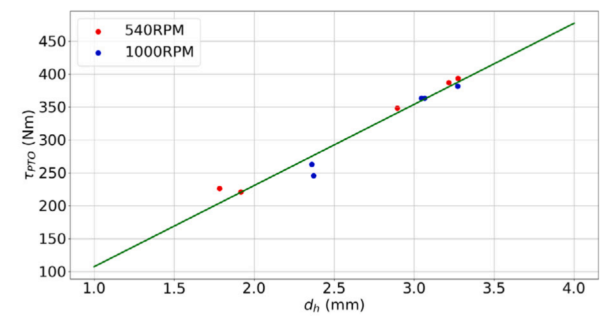

(b) Chain B (R^2 = 0.98).

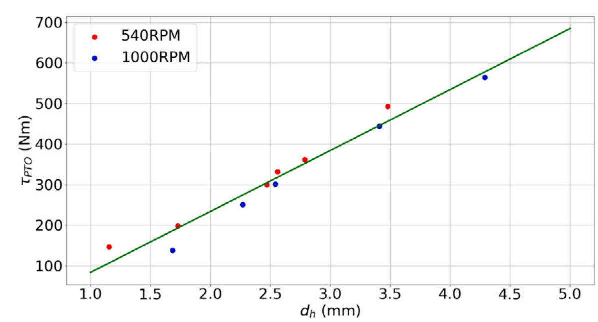

(c) Chain C (R^2 = 0.98).

Fig. 9. Torque range and rotary sensor horizontal displacement scatter plots for static indoor testing completed with chains A,B, and C.

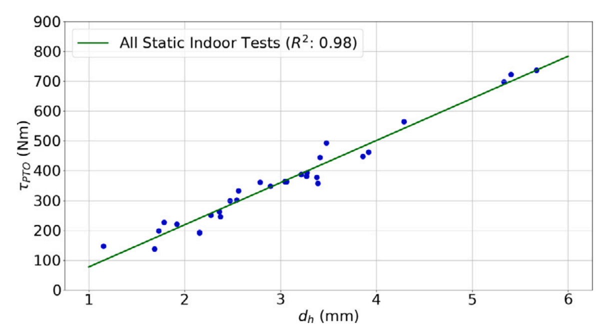

Fig. 10. Torque range and rotary sensor horizontal displacement scatter plots for all static indoor chain tests.

3.3. In-field implement baling experiments results

This section examines how τ_{CR} and main chain drive elastic extension is affected by the baling of grass silage crop. τ_{CR} and sprocket arm movement data were collected from a McHale Fusion 3+ baler-wrapper

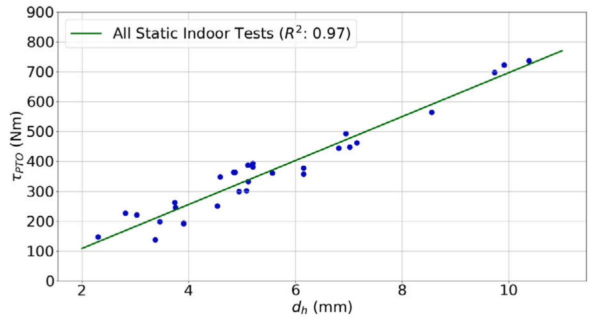

Fig. 11. Torque range and modelled ee_{chain} scatter plots for all static indoor chain tests.

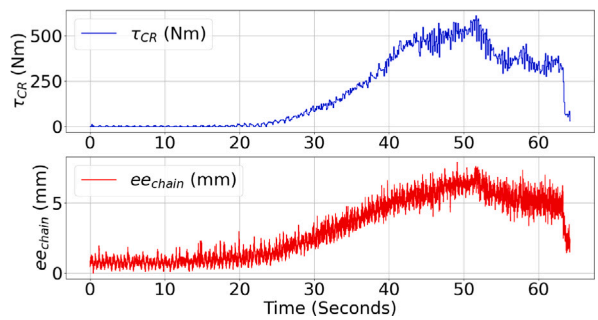

Fig. 12. τ_{CR} and ee_{chain} for one in-field silage bale cycle.

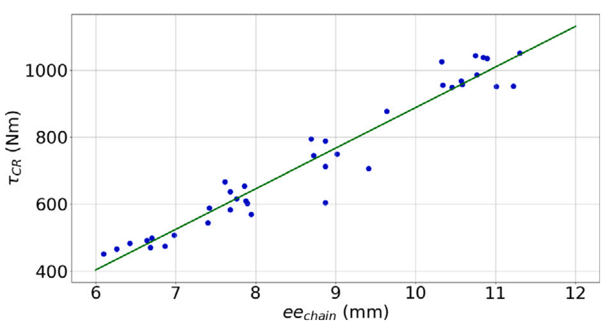

Fig. 13. Scatter plot of τ_{CR} correlated with chain elastic stretch found from in-field baling of 42 bales yielded an $R^2 = 0.97$.

during the baling of one field as described in Section 2.2.2. Peak τ_{CR} and corresponding chain drive elastic stretch are correlated during the formation of each bale. An example of ee_{chain} and τ_{CR} for one bale cycle is shown in Fig. 12. Peak τ_{CR} and ee_{chain} from the 42 bales made during in-field testing are correlated and shown in Fig. 13.

The OLS fit for in-field experiments, correlated τ_{PTO} range and main chain drive elongation data registered a significant R^2 coefficient of 0.97. In-field testing showed that τ_{CR} was estimated using main chain drive elongation during bale harvesting with a significant correlation with an R^2 value.

3.4. Full season silage baling analysis

In this section, the study examines both the permanent plastic (Section 3.4.1) and elastic (Section 3.4.2) main chain drive elongation throughout an entire season of grass harvesting, as described in Section 2.2.3. The method used to collect data and approximate torque using chain length data acquired during a full season of silage harvesting is explained in Section 2.2.3.

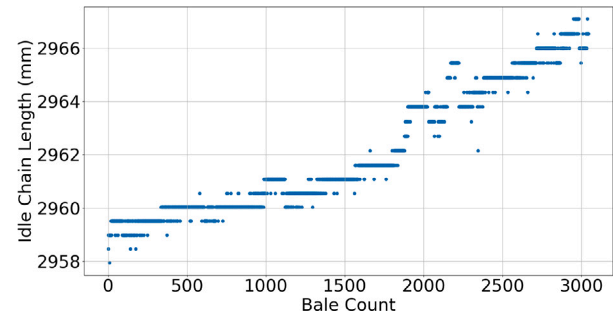

Fig. 14. Chain length due to plastic elongation throughout the full harvest season.

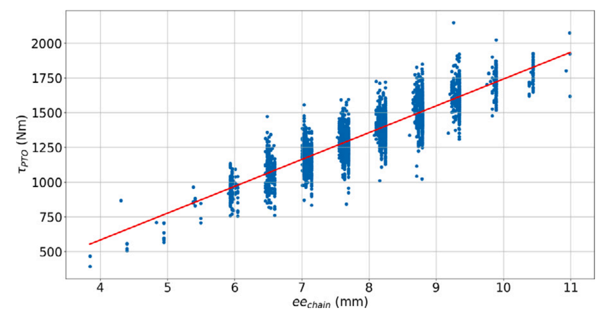

Fig. 15. Bale torque and main chain drive elongation correlation for 3001 bale cycles during full harvest season experiments yielded an $R^2 = 0.88$.

3.4.1. Chain permanent plastic elongation

Analysis of idle chain length during the full silage harvest season showed that as the season progressed and the bale count increased, the main chain drive, gradually stretched due to wear of chain components as described in Section 1. Plastic elongation is illustrated by plotting chain length estimated from the tensioner sprocket arm position during the initial idle stage of each bale cycle against the bale count throughout the season, as shown in Fig. 14.

3.4.2. Chain elastic elongation

During a full season of silage harvesting experiments the ground truth torque measurement was taken from the tractor PTO (τ_{PTO}), and included contributions from both τ_{PU} and τ_{CR}. The presence of τ_{PU} caused fluctuations in torque readings. To counter this, a median filter was applied to baler torque signals for each bale as the filtered torque signal more closely resembled τ_{CR}. The peak median filtered torque for each of the 3001 bale cycles under analysis were correlated with ee_{chain} for each bale and results are shown in Fig. 15.

The R^2 coefficient of 0.88 is observed between ee_{chain} and τ_{PTO} during the full silage harvesting season experiment. This is lower than the R^2 coefficient during static indoor implement and in-field implement experiments, described in Sections 3.2 and 3.3, respectively. This may be caused by the presence of τ_{PU} in the bale cycle torque measurement throughout the season. The rotary sensor can only determine the elastic stretch for the τ_{CR}, whereas τ_{PU} cannot be accounted for and may cause the variance, evident in Fig. 15.

The angular resolution of the rotary sensor used during season long testing was 0.3 degrees. The angular resolution was lowered due to limitations with the data acquisition hardware and ECU resources, causing space between groups of ee_{chain} data across the x-axis evident in Fig. 15. Within these groups of ee_{chain} data, further gaps present between vertical data points as illustrated in Fig. 16, where columns of points present around a specific ee_{chain} measure on the x-axis. These smaller gaps between groups of data are not caused by sensor resolution, but by plastic elongation of the chain throughout the harvest season as in Fig. 14. Fig. 16 shows how ee_{chain} increases within the data

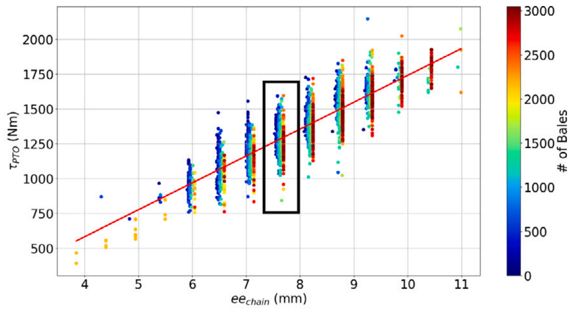

(a) Bale torque and ee_{chain} correlation during full harvest season testing, the colour of the data increases from blue to red as the number of bales made increases during the harvest season.

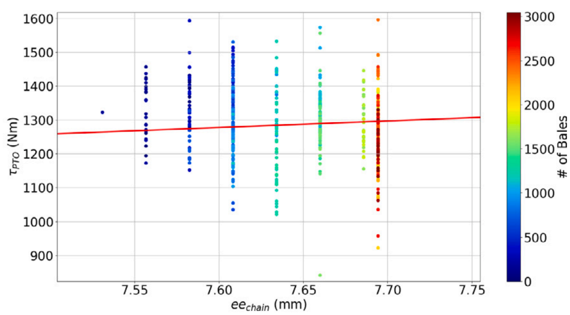

(b) Zoomed in image of data group in Figure 16a illustrating the increase in ee_{chain} as the number of bales made throughout the harvest season.

Fig. 16. Bale torque and ee_{chain} correlation during full harvest season testing with data highlighted based on bale count during the year.

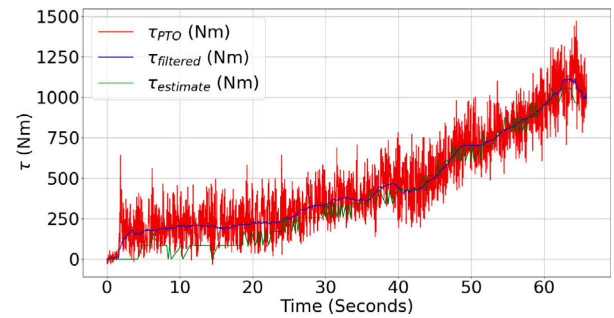

Fig. 17. Measured baler torque (τ_{PTO}), median filtered baler torque ($\tau_{filtered}$) and estimated torque ($\tau_{estimate}$) for one bale cycle. Average bale cycle error = 66 Nm, Bale compaction period of the bale cycle error = 34 Nm, Torque peak error = 60 Nm.

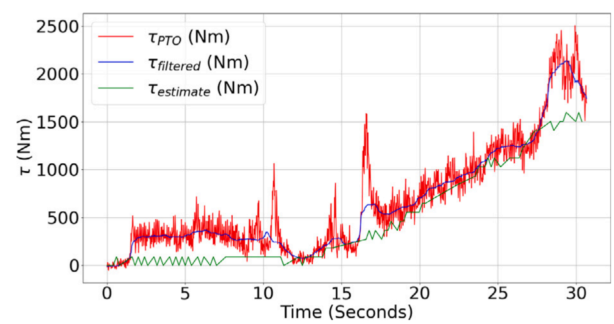

Fig. 18. Measured baler torque (τ_{PTO}), median filtered baler torque ($\tau_{filtered}$) and estimated torque ($\tau_{estimate}$) for one bale cycle. Average bale cycle error = 166 Nm, bale compaction error = 179 Nm, and peak torque error = 538 Nm. High peak torque error may be caused by increased τ_{PU} at the final stage of the bale cycle due to crop entering the bale chamber.

group, as the amount of bales made throughout the season increases. In Fig. 16(b), the bales made at the beginning of the year are shown in navy blue, while the bales made towards the end of the season are in red. As the chain stretches due to plastic elongation throughout the year, ee_{chain} gradually increases.

While the change in θ_{rs} may be the same during a bale cycle at the beginning and the end of the season long test, as θ_{rs} increased due to plastic elongation, ee_{chain} increases when converting θ_{rs} to chain length. For example, a bale made at the beginning of the year with an idle θ_{rs} of 80°and maximum θ_{rs} of 85°would have a same change in θ_{rs} as a bale made at the end of the year with an idle θ_{rs} of 85°and maximum θ_{rs} of 90°. However, due to a non linear relationship between ee_{chain} and rotary angle sensor data, as illustrated in Fig. 8, the bale made at the beginning of the year would have a lower ee_{chain} value.

3.4.3. Torque estimation

The season-long harvest data were used to estimate baler torque, as explained in Section 2.2.3. Figs. 17 and 18 show the measured baler torque, median filtered baler torque and torque estimated using ee_{chain} data for separate bale cycles, as in Eq. (3). Estimated torque is compared with the ground truth filtered torque cycle for 3001 valid bales. The error metrics outlined in Section 2.2.3 are calculated across the dataset and presented in Table 1.

Results show that $\tau_{filtered}$ during the bale compaction of the bale cycle can be estimated with an error of 8% and peak $\tau_{filtered}$ can be estimated with an error of 5% using ee_{chain}. The significant error percentages found from entire bale cycle estimation metrics are due to high levels of error during the initial period of each bale cycle, due to the dominance of τ_{PU} in τ_{PTO} with τ_{PU}, not accounted for in ee_{chain} torque estimations as explained in Section 2.1.1. The results indicate that chain length data can effectively estimate baler torque during the final stage of the baling cycle, a point at which the likelihood of slip clutch occurrences is greatest. These estimations can potentially be used by a machine operator to alter their driving behaviour to prolong the lifespan of the machinery, prevent blockages and, more crucially, reduce the risk of an unscheduled breakdown during a busy harvesting period.

3.5. In-field and season experiment comparisons

In this section, the torque range and main drive chain length relationship during in-field and harvest season experiments are compared. Static indoor test results were not compared with in-field and season test results as, unlike the other tests completed, no grass was harvested during indoor testing and force was applied to the baler chamber with a brake instead of grass inside the chamber.

Fig. 19 illustrates peak torque displacement correlated with chain length for in-field and season long experiments. Data from each test is multiplied by a ratio depending on the baler gearbox used during that test. Both 540 and 1000 RPM machines were used during the two test scenarios.

When full harvest season results are compared with in-field experiment results, the slope of the line of best fit in each experiment is similar, illustrating that as τ_{CR} increases, the rate of chain length increase is the same during both experiments. There is a consistent vertical gap between the OLS fit for full harvest data and the OLS fit for in-field experimental data. The difference in magnitude may be explained by the torque measurements over the full season being taken from the PTO shaft which includes both τ_{CR} and τ_{PU}. This additional τ_{PU} cannot be accounted for using the proposed solution which may increase the variance of measurements at particular x-axis locations as well as account for the magnitude difference between the OLS fits.

Table 1
Season testing results.

Season Testing Results			
Bale Sequence Metric	Bale Cycle Error	Bale Compaction Period Error	Torque Peak Error
Mean Error (Nm)	98	87	86
Median Error (Nm)	94	73	71
Maximum Error (Nm)	306	366	538
Minimum Error (Nm)	26	21	0
Standard Deviation	32	49	69
Mean Error (%)	195	11	7
Median Error (%)	82	8	5

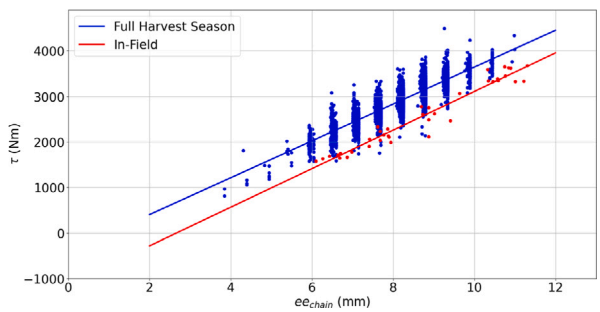

Fig. 19. In-field and Season baler torque experiment comparisons.

3.6. Study limitations

In the static indoor testing scenario outlined in Section 2.2.1, a brake unit was fitted to a single roller cylinder of a Fusion 3+ baler. This action exerted a load on the baler's main drive chain system, resulting in the displacement of the tensioning sprocket, as illustrated in Figs. 3 and 4.

The maximum load was constrained by the physical hydraulic pressure applied to the brake system and the wear of the brake pads, with excessive load occasionally causing pad ignition (Fig. 5). Consequently, the maximum torque recorded was approximately 730 Nm, as detailed in Section 3.2, which is significantly below the overload slip clutch threshold of 2000 Nm for a 540RPM Fusion3+. It is important to note that such artificial loading (on a single CR roller) may not accurately represent the forces exerted on multiple rollers when a cylindrical silage bale, weighing between 500 kg and 700 kg, rotates within the CR.

During the in-field tests described in Sections 3.3 and 2.2.2, the rotating mass of silage fodder within the chamber generated torque on the CR driveshaft. This torque was measured using a customized Fusion 3+ baler equipped with a torque sensor exclusively on the CR driveshaft. In contrast, measured torque from the static indoor tests (Section 2.2.1) and the season-long testing (Section 2.2.3) originated from a sensor installed on the PTO shaft. These measurements reflect loading contributions from both the CR and PU of the baler; however, the proposed method does not account for crop intake at the PU. This discrepancy is not an issue for the indoor scenario, however, the PU loading likely contributed to the variance in peak PTO torques shown in Fig. 16(a).

Additionally, significant mechanical design changes between the 2013 Fusion 3+ baler used during the entire harvest season (Section 3.4) and the 2021 model, used for generating in-field results (Section 3.3), may account for the discrepancies in the OLS fits presented in Fig. 19.

Future work will focus on reducing these inconsistencies and constraints by refining measurement techniques to more accurately capture the forces exerted on the multiple rollers during bale rotation within a static artificial loading scenario. A prototype machine will be used by a contractor to generate a novel dataset, with the customized ground-truth CR torque sensor used in Section 2.2.2 to mitigate the contributions from the PU. Additionally, exploring advanced sensor technologies and integrating them with machine learning algorithms could provide more accurate models.

4. Conclusions

In this paper, a novel bolt-on sensor solution was developed to measure implement power requirements on a round baler. The elastic chain elongation was observed during a loading sequence and a relationship was established with the input driveshaft torque of the gearbox. The relationship is then used to provide an estimate of the chamber power loading requirements of the baler.

Static, in-field and full silage harvesting season experiments were carried out where a fixed chamber baler torque and chain length were recorded. Several Power-Take-Off speeds and implement chain designs were evaluated while a controlled load was applied to the baler chamber rollers during static testing. In-field measurements were acquired during supervised baling experiments, and then over a full harvesting season, where data was acquired for 3001 bale formations.

The peak torque requirements of the chamber are shown to exhibit a linear correlation ($R^2 \geq 0.97$) with the elastic chain elongation during static and in-field supervised testing. During harvest season testing, the correlation coefficient was 0.88, with variation attributed to ground-truth power measurements reflecting a combination of chamber and crop pick-up components on the implement, a combination that cannot be accounted for with the proposed method. Despite this, the season baling results show that filtered peak torque can be estimated with a median error of 5%.

The paper contributes a method that approximates input power requirements on a chain driven bling implement while reducing the financial cost by an order of magnitude, when compared to the state-of-the-art. The output form the method could provide operators with real-time feedback on their implement loading, allowing them to improve their baling efficiency and reduce crucial component wear and downtime in the field. The paper examines the limitations of the technique, highlighting the difference in model fit, when comparing baling implements that are artificially loaded and those that are producing bales, in the field. Future development should focus on validating the method across a broader range of fixed chamber balers and analysing power requirements for different crop types including hay, straw, and miscanthus.

CRediT authorship contribution statement

Tomás Crotty: Writing – review & editing, Writing – original draft, Visualization, Validation, Software, Methodology, Investigation, Formal analysis, Data curation, Conceptualization. **John Warren:** Supervision, Resources, Methodology, Formal analysis, Funding acquisition, Conceptualization. **Conor Shanahan:** Writing – review & editing, Supervision, Project administration, Resources, Methodology, Formal analysis, Funding acquisition, Conceptualization. **Edward Jones:** Supervision, Resources, Funding acquisition, Conceptualization. **Martin Glavin:** Writing – review & editing, Supervision, Resources, Project administration, Funding acquisition, Conceptualization. **Dallan Byrne:** Writing – review & editing, Supervision, Methodology, Investigation, Data curation, Visualization, Validation, Software, Formal analysis, Funding acquisition, Conceptualization, Project administration.

Declaration of competing interest

The authors declare the following financial interests/personal relationships which may be considered as potential competing interests: Dallan Byrne reports financial support was provided by University of Galway. Tomas Crotty reports financial support was provided by University of Galway. John Warren reports financial support was provided by McHale Engineering Unlimited Company. Conor Shanahan reports financial support was provided by McHale Engineering Unlimited Company. Martin Glavin reports financial support was provided by University of Galway. Edward Jones reports financial support was provided by University of Galway. Dallan Byrne, Tomas Crotty, Martin Glavin, Edward Jones, John Warren, Conor Shanahan has patent EP4388864A1 "A baler and a method for determining the power drawn by a bale chamber of a baler and a method for determining the quantity of material in a bale chamber and for determining the optimum ground speed for the baler" pending to McHale Engineering Unlimited Company and the University of Galway. If there are other authors, they declare that they have no known competing financial interests or personal relationships that could have appeared to influence the work reported in this paper.

Acknowledgements

This work was supported by Lero and McHale Engineering Unltd. with financial support of Taighde Éireann – Research Ireland under Grant number 13/RC/2094_2 and by the Enterprise Ireland Marie Skłodowska-Curie Career-FIT Fellowship (Grant number MF-2018-0202).

Data availability

The data that has been used is confidential.

References

Balmos, A.D., Castiblanco, F.A., Neustedter, A.J., Krogmeier, J.V., Buckmaster, D.R., 2022. ISOBlue avena: A framework for agricultural edge computing and data sovereignty. IEEE Micro 42 (1), 78–86. http://dx.doi.org/10.1109/MM.2021.3134830.

Beirle, S., Seemann, K., 2020. Non-contact high-frequency measurements of mechanically loaded ferromagnetic thin films: An alternative approach for torque sensors. Sensors Actuators A- Phys. 301, 111788. http://dx.doi.org/10.1016/j.sna.2019.111788.

Brodie, S., Oksanen, T., Auernhammer, H., 2023. Buzzword ISOBUS. Inform. Spektrum 46 (1), 46–50. http://dx.doi.org/10.1007/s00287-022-01518-4.

Brüel, H., Kjær, 2022. Methods of torque measurement in drive train technology. URL: https://www.hbm.com/en/3706/tips-and-tricks-torque-measurement-methods/.

Buckmaster, D., 2003. Benchmarking tractor costs. Appl. Eng. Agric. 19 (2), 151–154. http://dx.doi.org/10.13031/2013.13104.

Calian Advanced Technologies, 2020. Dual feed GNSS antenna - pre-filtered TW4422. URL: https://www.calian.com/advanced-technologies/gnss_product/tw4422-single-band-gnss-antenna-pre-filtered/. 770 Palladium Dr. 4th floor, Ottawa, ON Canada K2V 1C8.

Cory, B., 2005. Belt, rope and chain drives. In: Fans and Ventilation. Elsevier Science, Oxford, pp. 177–185. http://dx.doi.org/10.1016/B978-008044626-4/50013-9.

Creo, 2022. Pro/ENGINEER Software website. URL: http://www.proengineer.com/.

Diamond-Drives, 2024. Diamond-drives: Precision roller chain manufacturer. URL: https://www.diamonddrives.com/. 901 19th Avenue, Fulton, Illinois 61252.

Emlid, 2020. Reach M2 and M+ - RTK GNSS/GPS modules for high precision mapping. URL: https://emlid.com/reach/. (Accessed: 12 February 2024).

Fasick, G.T., Liu, J., 2020. Lab scale studies of miscanthus mechanical conditioning and bale compression. Biosyst. Eng. 200, 366–376. http://dx.doi.org/10.1016/j.biosystemseng.2020.10.011.

Finch, H., Samuel, A., Lane, G., 2014. Lockhart & Wiseman's Crop Husbandry Including Grassland, Conservation of Grass and Forage Crops, nineth ed. Elsevier, URL: https://www.sciencedirect.com/book/9781782423713/lockhart-and-wisemans-crop-husbandry-including-grassland.

Genever, L., 2019. Making Grass Silage for Better Returns. Technical Report, UK Agriculture and Horticulture Development Board, URL: https://ahdb.org.uk/knowledge-library/making-grass-silage-for-better-returns.

Grandovska, B., Cook, E., Rybkowska, A., Selenius, J., 2018. Farm Structure Survey 2016. Technical Report, European Commission EUROSTAT, URL: https://ec.europa.eu/eurostat/documents/2995521/9028470/5-28062018-AP-EN.540pdf/8d97f49b-81c0-4f87-bdde-03fe8c3b8ec2.

Harkin, S.J., Crotty, T., Warren, J., Shanahan, C., Jones, E., Glavin, M., Byrne, D., 2024. Field-to-field coordinate-based segmentation algorithm on agricultural harvest implements. IEEE Trans. AgriFood Electron. 2 (1), 91–104. http://dx.doi.org/10.1109/TAFE.2024.3352480.

Hoffmann, S., 2018. Bale forming apparatus and method with overload protection. (US10034432B2).

Hofstetter, D., Liu, J., 2011. Power requirement and energy consumption of bale compression. In: American Society of 526 Agricultural and Biological Engineers Annual International Meeting 2011, Vol. 7, No. 11. ASABE 2011, pp. 5401–5413. http://dx.doi.org/10.13031/2013.38496.

HYDAC, 2022. Portable Data Recorder HMG 4000 Operating Manual. URL: https://www.hydac.com/shop/en/hmg-4000-twelve-measurement-inputs-analogue-digital-hsi-sensors-can-and-io-link-interface-1000536076. Industriestraße, 66280 Sulzbach/Saar, Germany.

Keles, G., O'Kiely, P., Lenehan, J., Forristal, P., 2009. Conservation Characteristics of Baled Grass Silages Differing in Duration of Wilting, Bale Density and Number of Layers of Plastic Stretch-Film. Teagasc, Oak Park, Carlow, Ireland, URL: http://hdl.handle.net/11019/646.

Lei, J., Wang, S., 2021. Mechanical properties of steel-roll round baler during the baling process. In: 2021 6th International Conference on Intelligent Information Processing. ACM, Bucharest Romania, pp. 299–304. http://dx.doi.org/10.1145/3480571.3480625.

Lyons, W.C., Plisga, G.J., Lorenz, M.D., 2016. Auxiliary equipment. In: Standard Handbook of Petroleum and Natural Gas Engineering (Third Edition), third ed. Gulf Professional Publishing, Boston, 3–1–3–66. http://dx.doi.org/10.1016/B978-0-12-383846-9.00003-5.

McHale, P.C., Mchale, M.W., McHale, P.G., Biggins, J.P., Warren, J.A., Shanahan, C.P., Heaney, J.J., 2024. A baler and a method for baling material. (WO2024231910A2), URL: https://worldwide.espacenet.com/patent/search/family/093431879/publication/WO2024231910A2?q=pn%3DWO2024231910A2.

Mohsenimanesh, A., Nieuwenhof, P.P., Necsulescu, D.D., Laguë, C., 2015. Monitoring of a forage harvester using multiple sensor fusion. In: American Society of Agricultural and Biological Engineers Annual International Meeting 2015, Vol. 1, No. January 2016. pp. 727–732. http://dx.doi.org/10.13031/aim.20152179904.

Muck, R.E., Shinners, K.J., 2021. Conserved forage (silage and hay): progress and priorities. In: IGC Proceedings (1993-2023), No. 24. URL: https://uknowledge.uky.edu/igc/19/21/24.

NCTE AG, 2020. Torque Sensor Series 3000 Instruction Manual and Data Sheet. Technical Report, NCTE, URL: https://ncte.com/wp-content/uploads/2021/01/Instruction_manual_data_sheet_series3000_EN_V20_02.pdf. Raiffeisenallee 3, 82041 Oberhaching, Germany.

Nienhaus, C., 2012. Overload Clutches and Designs in Agritechnical Engineering – from the Beginnings to the Present Day. VDI Landtechnik, pp. 374–384, URL: https://www.agricultural-engineering.eu/landtechnik/article/download/2012-67-5-374-384/2012-67-5-374-384-en-pdf/538.

Niijjaawan, N., Niijjaawan, R., 2010. Steel wire and chain. In: Modern Approach To Maintenance in Spinning. Woodhead Publishing India, pp. 223–241. http://dx.doi.org/10.1533/9780857094056.223.

Otoshi, K., Kanehira, M., Otani, T., Yoshikawa, M., Takahashi, T., 1995. The Complete Guide to Chain. Sachio Shimura, URL: http://chain-guide.com/.

Parvin, N., Coucheney, E., Gren, I.-M., Andersson, H., Elofsson, K., Jarvis, N., Keller, T., 2022. On the relationships between the size of agricultural machinery, soil quality and net revenues for farmers and society. Soil Secur. 6, 100044. http://dx.doi.org/10.1016/j.soisec.2022.100044.

Regler, F., Hausmann, F., Krüger, M., Bernhardt, H., 2023. Potential and improvement of maintenance efficiency of agricultural PTO shafts by a new digital maintenance assistant. Agriculture 13 (2), 227. http://dx.doi.org/10.3390/agriculture13020227.

U-Blox, 2020. UBLOX NEO-M8 series. URL: https://www.u-blox.com/en/product/neo-m8-series. Zürcherstrasse 68, Thalwil, 8800, Switzerland.

Van Middelaar, C., Dijkstra, J., Berentsen, P., De Boer, I., 2014. Cost-effectiveness of feeding strategies to reduce greenhouse gas emissions from dairy farming. J. Dairy Sci. 97 (4), 2427–2439. http://dx.doi.org/10.3168/jds.2013-7648.

Wilkens, D.D., Honhold, J., Roehrbein, J., 2002. Round baler for agricultural procedure. (EP0855134B1), URL: https://worldwide.espacenet.com/patent/search/family/007817589/publication/EP0855134B1?q=EP0855134B1.

Wilkinson, J.M., 1981. Losses in the conservation and utilisation of grass and forage crops. Ann. Appl. Biol. 98, 365–375. http://dx.doi.org/10.1111/j.1744-7348.1981.tb00769.x.